J Mol Model (2013) 19:601–611
DOI 10.1007/s00894-012-1588-8

ORIGINAL PAPER

# Cyclo-hexa-peptides at the water/cyclohexane interface: a molecular dynamics simulation

**Min Cen · Jian Fen Fan · Dong Yan Liu · Xue Zeng Song · Jian Liu · Wei Qun Zhou · He Ming Xiao**

Received: 14 February 2012 / Accepted: 28 August 2012 / Published online: 16 September 2012


**Abstract** Molecular dynamic (MD) simulations have been performed to study the behaviors of ten kinds of cyclo-hexa-peptides (CHPs) composed of amino acids with the diverse hydrophilic/hydrophobic side chains at the water/cyclohexane interface. All the CHPs take the "horse-saddle" conformations at the interface and the hydrophilicity/hydrophobicity of the side chains influences the backbones' structural deformations. The orientations and distributions of the CHPs at the interface and the differences of interaction energies ($\Delta\Delta E$) between the CHPs and the two liquid phases have been determined. RDF analysis shows that the H-bonds were formed between the $O_C$ atoms of the CHPs' backbones and $H_w$ atoms of water molecules. N atoms of the CHPs' backbones formed the H-bonds or van der Waals interactions with the water solvent. It was found that there is a parallel relationship between $\Delta\Delta E$ and the lateral diffusion coefficients ($D_{xy}$) of the CHPs at the interface. The movements of water molecules close to the interface are confined to some extent, indicating that the dynamics of the CHPs and interfacial water molecules are strongly coupled.

**Keywords** Cyclo-hexa-peptides (CHPs) · Hydrophilicity/hydrophobicity · MD · Water/cyclohexane interface

**Electronic supplementary material** The online version of this article (doi:10.1007/s00894-012-1588-8) contains supplementary material, which is available to authorized users.

M. Cen · J. F. Fan (✉) · D. Y. Liu · X. Z. Song · W. Q. Zhou
College of Chemistry, Chemical Engineering and Materials Science, Soochow University,
Suzhou 215123, People's Republic of China
e-mail: jffan@suda.edu.cn

J. F. Fan
e-mail: jffan1305@163.com

J. Liu
Shanghai Institute of Applied Physics,
Chinese Academy of Sciences,
PO Box 800–204, Shanghai 201800, People's Republic of China

H. M. Xiao
College of Chemical Engineering,
Nanjing University of Science and Technology,
Nanjing 210094, People's Republic of China

## Introduction

Cyclic peptides characterized with the closed ring structures can be formed by even alternating *D*- and *L*- amino acids linked end to end. These species exhibit various biological activities, such as antibacterial [1], antiviral [2], antifungal [3], immunosuppressant [4] and antinociceptive properties [5]. Their amphiphilic characteristics make them to be potential superior candidates of surfactants [6]. Besides, cyclic peptides can self-assemble into peptide nanotubes, as models of biological transmembrane channels [7]. Such surface and biological properties have attracted interest in the structures of cyclic peptides and their behaviors at the hydrophilic/hydrophobic interfaces.

The structures and ring sizes of cyclic peptides have major impacts on the peptides' biological activities. Bagheri et al. [8] found that the antibacterial activities of the cationic antimicrobial peptides increase with the peptide hydrophobicity. It was reported that the cyclic cationic antimicrobial peptides with large rings show low amphiphilicity [9]. The structural and dynamical studies of all-trans and all-cis cyclo[(1R,3S)-γ-Acc-Gly]$_3$ peptides showed that the cavity of all-cis is able to conduct water molecules in a much better fashion than all-trans pore [10]. The significant binding energies of cyclo[(1R,3S)-c-Acc-Gly]$_3$ hexapeptide upon $Na^+$ and $K^+$ enclosures show that its nanotubular structure might act as an ion channel of biological interest [11].

A good estimation of the hydrophilicity/hydrophobicity is essential for understanding the behaviors of cyclic peptides at an interface or in a solution. Traditionally, the hydrophilic/hydrophobic interaction was obtained approximately through the calculation of the migration energy of a solute between aqueous and oil phases [12, 13]. Horinek

group [14] proposed a method to quantitatively predict the free energy of a peptide transferring to a urea solution.

Surface activity mainly occurs at interfaces and is governed by the conformational state of molecules at the hydrophobic/hydrophilic interface. 3-D conformation of the peptide ring was characterized to adopt a "horse-saddle" at the water/hexane [15], water/decane interfaces [6] and in DMSO solution [16]. It was reported that the folded conformation corresponds to the most stable amphipathic structure determined by NMR [17]. The two acidic amino acid residues were close to each other and formed a hydrophilic domain on one side of the molecule, and the hydrophobic domain on the opposite side was populated by the aliphatic chain and most of the hydrophobic amino acid residues. It was reported that the conformations and dynamics of cyclic peptides at an interface depended on the nature of the hydrophobic/hydrophilic interface and the local interfacial concentration [18]. X-ray reflectivity study showed cyclic peptides preferentially adopt an orientation parallel to the air/water interface at low surface pressure, and continuous compression may cause the molecules to flip to a perpendicular state [19].

A variety of techniques have been applied to study the structures and properties of cyclic peptides, such as NMR, surface plasmon resonance, STM, infrared absorption spectrum technology and molecular dynamics (MD). The experimental distribution measurements encounter dissolution difficulties [20]. However, MD realizes the simulations of the structures and properties of the cyclic peptides with the different amino acid residues spontaneously and accurately at the ensemble average level. MD simulations show that individual cyclic peptide rings are rapidly adsorbed at an oil/water interface, lying with their molecular planes mostly parallel to the interface, where they further self-assemble [21]. A lower temperature may contribute to a stronger tendency of cyclic peptides to aggregate at the interface [22].

The diverse types and amounts of the component amino acid residues develop the abundant structures and properties of cyclic peptides [23]. This work focuses on ten cyclohexa-peptides (CHPs) composed of amino acids with the diverse hydrophilic/hydrophobic side chains. Only the CHPs composed of single types of amino acid residues were chosen to be simulated for conciseness. The water/cyclohexane medium was employed to mimic the biological water/lipid biphasic system. The structures, orientations, distributions and dynamics of ten CHPs at the water/cyclohexane interface were investigated by MD simulations. The results give insights to the hydrophilicity/hydrophobicity and interfacial behaviors of cyclic peptides, which directly influence the peptide biological activities and self-assembly behaviors. This work is essential for our later self-assembly of cyclic peptides to produce peptide nanotubes (PNTs) with diverse external characteristics.

## Materials and simulation details

On the basis of our earlier work [24], ten kinds of CHPs formed by alternating *D*- and *L*- amino acids with diverse hydrophilic/hydrophobic side chains, shown in Fig. 1, were constructed. MD simulations were run with the Materials Studio 4.4 software, using the COMPASS force field with condensed-phase optimized molecular potentials [25].

All of the systems prepared for MD simulations have similar setup steps. First, two boxes with the same $L_x$ and $L_y$ lengths, containing 808 water and 105 cyclohexane molecules, respectively, were constructed and equilibrated for 10 ns with a time step of 1 fs in the NPT ensembles. The final densities of the two solvent boxes are 1.0 and 0.774 g/cm$^3$, respectively, which are in good agreement with the experimental values at the temperature of 298 K [26]. The two boxes were then placed side by side along the *z* direction with a small vacuum interstice of about 2 Å to eliminate possible overlap between them. After 5 ns equilibration, the dimensions of the simulation box in the *x*, *y* and *z* directions were 32.25, 32.25 and 45.75 Å, respectively. Our simulations showed that the asymmetry of the bi-phase system composed of water and cyclohexane phases may result in the migration of the water/cyclohexane interface, accompanied by the movement of a CHP molecule to the interface. The migration of the interface brought great complexity to the later analysis and data processing. Here, a graphene wall parallel to the water/cyclohexane interface was applied to solve the problem. It was set on the left side of the cell, far away from the interface in z direction and frozen just like a "wall" during the simulations. We have selectively

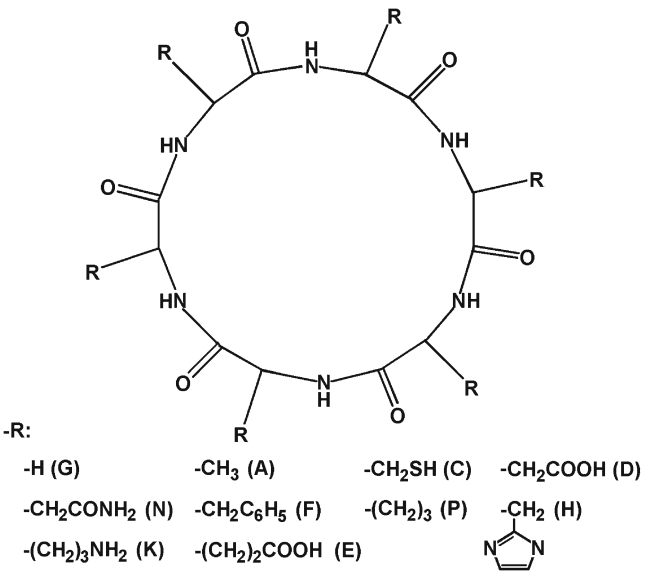


**Fig. 1** Scheme of the ten kinds of CHPs formed by even alternating *D*- and *L*- amino acids with the different hydrophilic/hydrophobic side chains. The letters in the parentheses stand for the abbreviations of the composed amino acids in the CHPs

simulated three CHPs in the systems with or without the graphene wall, and the diffusion results listed in the supplementary Table S1 show no distinct influences of the introduced graphene wall on the diffusion characteristics of CHPs at the interface. At last, a CHP molecule was positioned in the water or cyclohexane phase, 10 Å away from the interface. The periodic boundary conditions were applied in all three spatial directions. The temperature was controlled with the Nośe thermostat [27] and the pressure was maintained using the Berendsen method [28]. The atomic initial velocity was got from the random distribution of Maxwell-Boltzmann. Velocity verlet algorithm [29] was applied to solve the atomic Newton motion equation. Van der Waals interaction employed atom-based method. The Ewald summation method [30] was used for the electrostatic interaction. The cutoff radii of van der Waals and electrostatic interactions were both 9.5 Å. The spline and buffer widths were chosen as 1.0 and 0.5 Å, respectively.

The pre-equilibrium simulation was first done for the system in which all the $C_\alpha$ atoms of a CHP backbone were fastened. Energy minimization was further achieved for the system in which all the constraints on the CHP were eliminated. The 300 ps equilibration simulation was then performed at 298 K in the NPT ensemble with a small time step of 0.5 fs. Finally, 5 ns simulation was performed in the NVT ensemble with a time step of 1 fs and the trajectory was stored every 1 ps during the last 1 ns for analyzing the statistic and dynamic characteristics of the system.

## Results and discussion

### Structures of CHPs at the water/cyclohexane interface

Due to the amphiphilic characters, all the CHPs migrate to the water/cyclohexane interface, no matter their initial positions either in the water or cyclohexane phase. Simulations showed that a CHP molecule needs ~300 ps to migrate to the interface. It was found that all the backbones of CHPs adopt the "horse-saddle" conformations at the interface. Such "horse-saddle" structure can be characterized by the vectors of **CC** and **NN** of the backbone [15], illustrated in Fig. 2.

The vector lengths of |**CC**| and |**NN**| of CHPs are approximately 7.39 and 7.33 Å in gas phase, respectively. Distinct deformations of the CHPs at the water/cyclohexane interface occur, shown in Table 1. CHPs with the diverse hydrophilicity/hydrophobicity residues deform to different degrees. It was found that the cyclo-(PP)$_3$ peptide almost keeps a rigid planar structure, with the least conformational change. Nevertheless, the smallest cyclo-(GG)$_3$ peptide with no side chain exhibits the biggest deformation.

The relative deformation percentages (Δ|**CC**|% and Δ|**NN**|%) were investigated and depicted in Fig. 3. The total

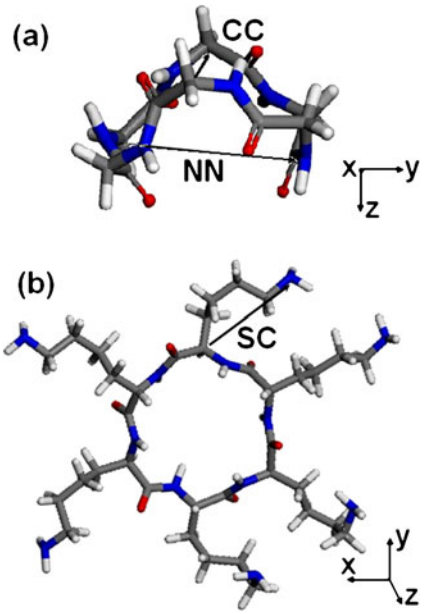


**Fig. 2** Schematic diagram of the **CC**, **NN** and **SC** vectors in the "horse-saddle" conformers of the two representative CHPs: (**a**) the cyclo-(GG)$_3$ peptide, (**b**) the cyclo-(KK)$_3$ peptide. **CC** vector was established between the two C atoms on the top of the "horse-saddle" in the reverse *x*-axis direction. **NN** vector was defined between the two N atoms on the bottom of the "horse-saddle" along the y-axis direction. **SC** vector was set from $C_\alpha$ atom of a backbone to the non-H atom at the end of a side chain

ones of the backbones were further computed by the sum of the absolute values of Δ|**CC**|% and Δ|**NN**|%. Δ|**CC**|% presents small positive values for the cyclo-(PP)$_3$, cyclo-(AA)$_3$, cyclo-(CC)$_3$ and cyclo-(FF)$_3$ peptides. However, it displays negative values for the cyclo-(NN)$_3$, cyclo-(DD)$_3$, cyclo-(KK)$_3$, cyclo-(GG)$_3$ and cyclo-(EE)$_3$ peptides. It is significant to characterize the hydrophilicity/hydrophobicity of

**Table 1** Average lengths (in Å) of the **CC, NN** and **SC** vectors and the lateral translational diffusion coefficients ($D_{xy}$ in $10^{-6}$cm$^2$·s$^{-1}$) of the CHPs at the water/cyclohexane interface

| CHPs | \|**CC**\| | \|**NN**\| | \|**SC**\|[a] | | *Dxy* |
|---|---|---|---|---|---|
| | | | Initial | Final | |
| Cyclo-(FF)$_3$ peptide | 8.50 | 7.27 | 5.11 | 5.12 | 3.711 |
| Cyclo-(CC)$_3$ peptide | 8.07 | 5.72 | / | / | 3.786 |
| Cyclo-(PP)$_3$ peptide | 7.68 | 7.57 | / | / | 3.750 |
| Cyclo-(AA)$_3$ peptide | 7.87 | 5.75 | / | / | 3.541 |
| Cyclo-(GG)$_3$ peptide | 6.43 | 5.27 | / | / | 3.602 |
| Cyclo-(DD)$_3$ peptide | 7.02 | 5.26 | 4.64 | 3.73 | 3.479 |
| Cyclo-(NN)$_3$ peptide | 7.31 | 5.57 | 4.59 | 2.4 | 3.426 |
| Cyclo-(KK)$_3$ peptide | 6.76 | 6.19 | 7.17 | 5.64 | 3.411 |
| Cyclo-(HH)$_3$ peptide | 7.40 | 6.09 | 5.45 | 5.36 | 3.353 |
| Cyclo-(EE)$_3$ peptide | 6.42 | 6.79 | 5.14 | 4.96 | 3.298 |

[a] The initial and final values represent the lengths of the **SC** vectors of CHPs in gas and at the water/cyclohexane interface, respectively

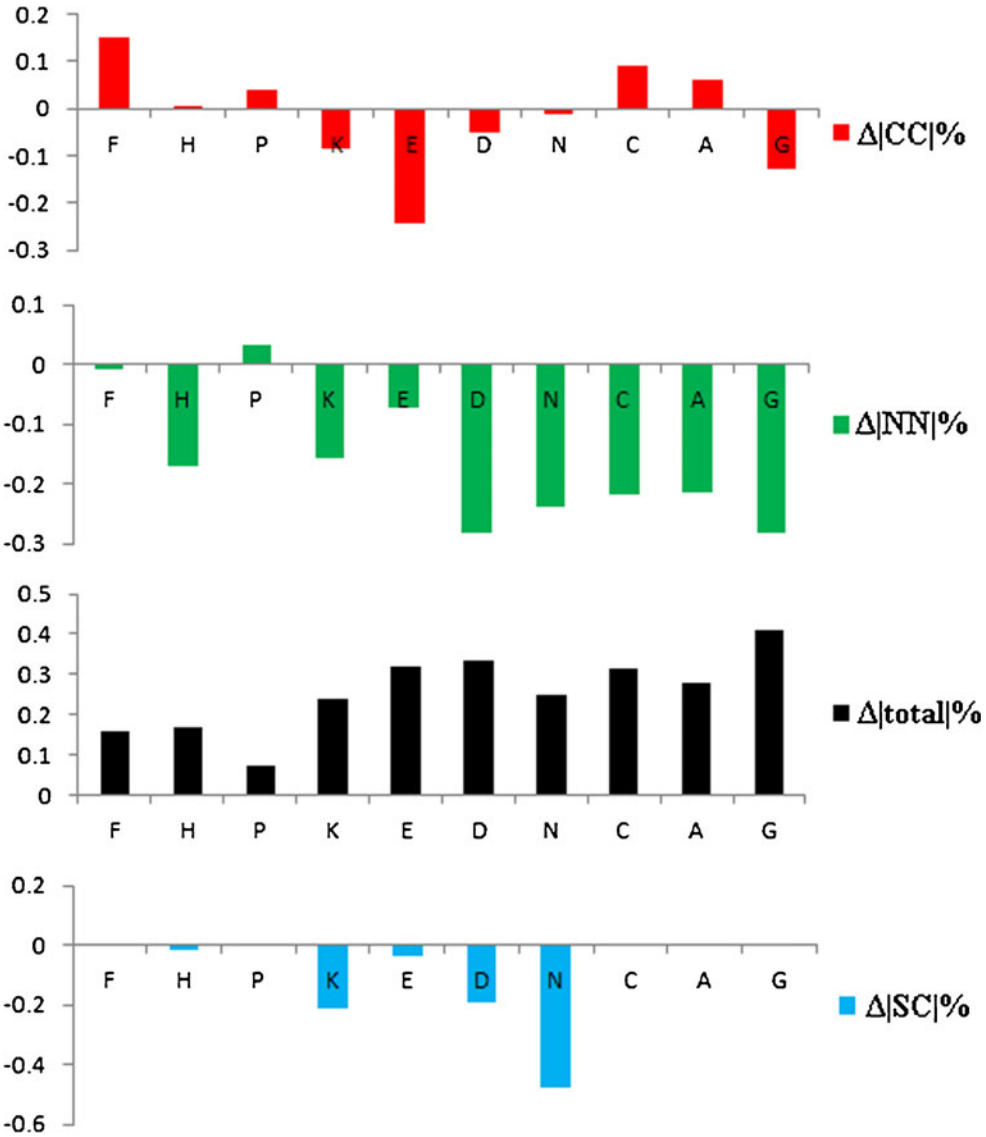


**Fig. 3** Relative deformation percentages (Δ|**CC**|%, Δ|**NN**|% and Δ|**SC**|%) and the total ones of CHP backbones, computed as the sum of the absolute values of Δ|**CC**|% and Δ|**NN**|%

CHPs. All the Δ|**NN**|% exhibits large positive values except for the cyclo-(P<u>P</u>)$_3$ peptide. The total deformation percentages in Fig. 3 show that the rigid ring structures of the side chains in the cyclo-(P<u>P</u>)$_3$, cyclo-(F<u>F</u>)$_3$ and cyclo-(H<u>H</u>)$_3$ peptides result in relatively small deformations of the backbones. However, great deformations were found in the other CHPs, mainly in the direction of **NN** vector, except for the cyclo-(E<u>E</u>)$_3$ peptide. The biggest deformation of the cyclo-(G<u>G</u>)$_3$ peptide also occurs in the direction of **NN** vector.

The relative deformation percentages of the side chains (Δ|**SC**|%) were analyzed and described in Fig. 3. The negative values of Δ|**SC**|% of the cyclo-(N<u>N</u>)$_3$, cyclo-(K<u>K</u>)$_3$, cyclo-(D<u>D</u>)$_3$ and cyclo-(E<u>E</u>)$_3$ peptides show that the side chains of these CHPs bend back to the CHP backbones. Further investigations show that the side chains of these CHPs interact with the backbones by the H-bonding formed between the end groups of the side chains and O, N atoms of the backbones.

## Orientations of CHPs at the water/cyclohexane interface

The orientations of CHPs at the water/cyclohexane interface were further investigated by measuring the angles between the vectors **R** (**R** indicates the **CC** or **NN** vector) in CHP backbones and the normal **n** to the water/cyclohexane interface plane (**n** directs from the cyclohexane to water phase). The orientational cosine is in the form of

$$\cos\alpha = \frac{\mathbf{R}\cdot\mathbf{n}}{|\mathbf{R}|} \quad (1)$$

Figure 4 depicts the normalized probability distributions of $\alpha_{CC}$. The main contributions of $\alpha_{CC}$ in the cyclo-(G<u>G</u>)$_3$, cyclo-(H<u>H</u>)$_3$ and cyclo-(P<u>P</u>)$_3$ peptides are about 80°, suggesting that the orientations of these CHPs tend to be parallel to the interface. These results are contributed to the absence of the side chain in the cyclo-(G<u>G</u>)$_3$ peptide or the rigid structures

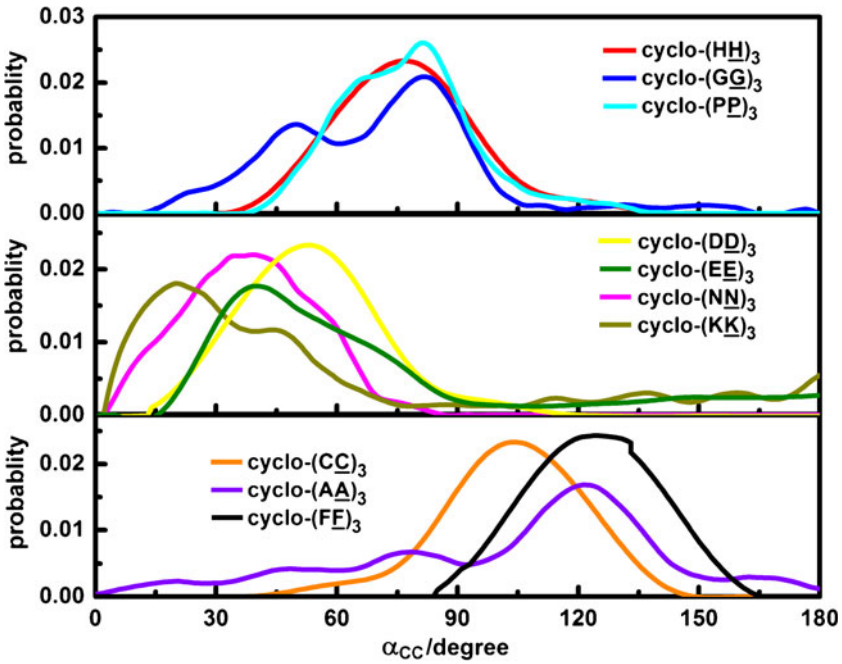


**Fig. 4** Normalized probability distributions of $\alpha_{CC}$, the orientation angles of the **CC** vectors in CHP backbones with respect to the normal **n** to the water/cyclohexane interface

of the side chains in the cyclo-(PP)$_3$ and cyclo-(HH)$_3$ peptides. The particular five-membered rings with two atoms of the backbone in the residues result in the relatively rigid cyclic structures of the side chains in the cyclo-(PP)$_3$ peptide. Similar rigid ring structures of the side chains in the cyclo-(HH)$_3$ peptide also exist. The main contributions of $\alpha_{CC}$ between 20 and 60° were observed for the cyclo-(DD)$_3$, cyclo-(EE)$_3$, cyclo-(NN)$_3$ and cyclo-(KK)$_3$ peptides. All these peptides display inserting into the aqueous phase. Nevertheless, the cyclo-(FF)$_3$, cyclo-(CC)$_3$ and cyclo-(AA)$_3$ peptides plug into the cyclohexane phase with the $\alpha_{CC}$ beyond 90°.

The grouping of the distributions of $\alpha_{NN}$, shown in Fig. 5, is similar to that of $\alpha_{CC}$. It is noteworthy that there are two distinct distribution peaks of $\alpha_{CC}$ and $\alpha_{NN}$ for the cyclo-(GG)$_3$ peptide with the largest backbone deformation (see Fig. 3). The highest peaks of $\alpha_{CC}$ and $\alpha_{NN}$ locate at about 80 and 50°, respectively, indicating that the largest deformation of the cyclo-(GG)$_3$ peptide mainly contributed

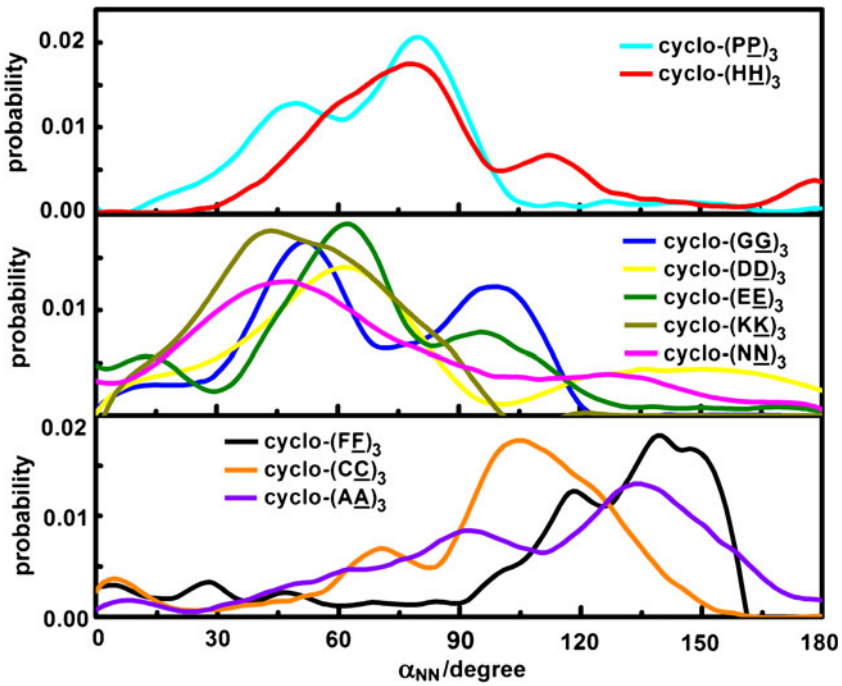


**Fig. 5** Normalized probability distributions of $\alpha_{NN}$, the orientation angles of the **NN** vectors in CHP backbones with respect to the normal **n** to the water/cyclohexane interface

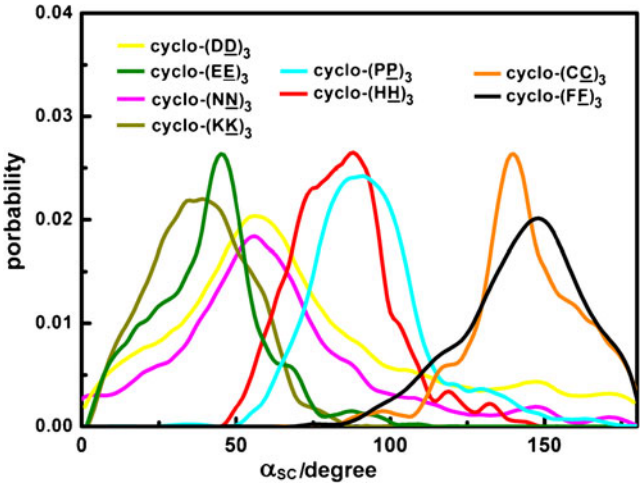


**Fig. 6** Normalized probability distributions of $\alpha_{SC}$, the orientation angles of the **SC** vectors in CHP side chains with respect to the normal **n to the water/cyclohexane interface**

by the shortening of **NN** vector relates with the tilt of **NN** vector at the interface.

The distributions of $\alpha_{SC}$ are shown in Fig. 6. The main distribution peaks of $\alpha_{SC}$ for the cyclo-(PP)$_3$ and cyclo-(HH)$_3$ peptides about 80° show that their rigid side chains mainly lay flat at the water/cyclohexane interface. For the cyclo-(DD)$_3$, cyclo-(EE)$_3$, cyclo-(NN)$_3$ and cyclo-(KK)$_3$ peptides with the hydrophilic side chains, the angles of $\alpha_{CC}$, $\alpha_{NN}$ and $\alpha_{SC}$ are all less than 90°, illustrating the inserting of these CHPs into the water phase. Such angles for the cyclo-(CC)$_3$, cyclo-(AA)$_3$ and cyclo-(FF)$_3$ peptides are all beyond 90°, due to the side chains' plugging into the cyclohexane phase.

## Concentration distributions of CHPs at the water/cyclohexane interface

Concentration profiles take atomic coordinates as input and plot the relative distributions of the specified atoms (or moieties) in layers parallel to the water/cyclohexane interface [31]. Concentration distributions of the backbone $C_\alpha$ atoms and some moieties in the side chains such as amino ($-NH_2$), hydroxyl ($-OH$), sulfydryl ($-SH$), C and N atoms were selectively analyzed and depicted in Fig. 7. The atoms in a side chain were numbered from the backbone to the end of the side chain in order. Those in the annular side chains of the cyclo-(PP)$_3$, cyclo-(FF)$_3$ and cyclo-(HH)$_3$ peptides were

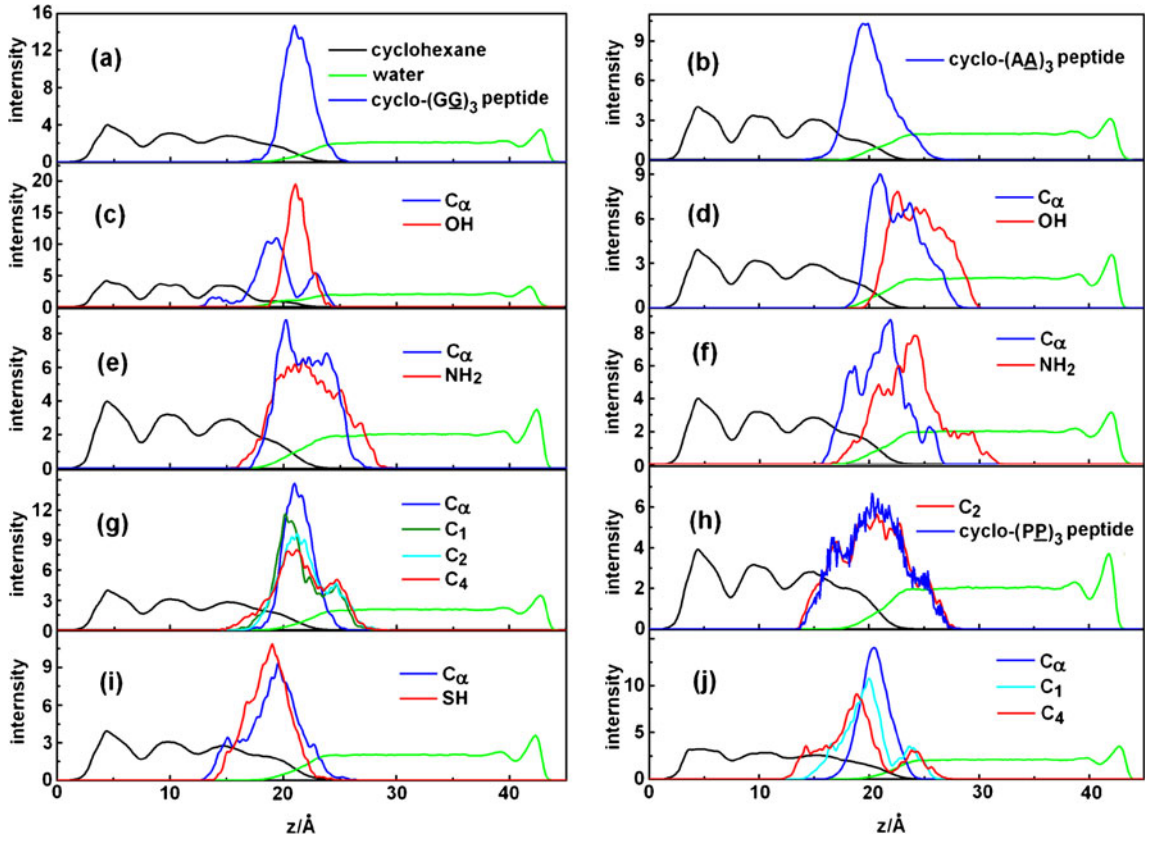


**Fig. 7** Concentration distribution profiles along *z*-axis of some selective moieties in the (**a**) cyclo-(GG)$_3$, (**b**) cyclo-(AA)$_3$, (**c**) cyclo-(DD)$_3$, (**d**) cyclo-(EE)$_3$, (**e**) cyclo-(NN)$_3$, (**f**) cyclo-(KK)$_3$, (**g**) cyclo-(HH)$_3$, (**h**) cyclo-(PP)$_3$, (**i**) cyclo-(CC)$_3$, (**j**) cyclo-(FF)$_3$ peptides. The atoms in a side chain were numbered from the backbone to the end of the side chain in order. Those in the annular side chains of the cyclo-(PP)$_3$, cyclo-(FF)$_3$ and cyclo-(HH)$_3$ peptides were numbered clockwise

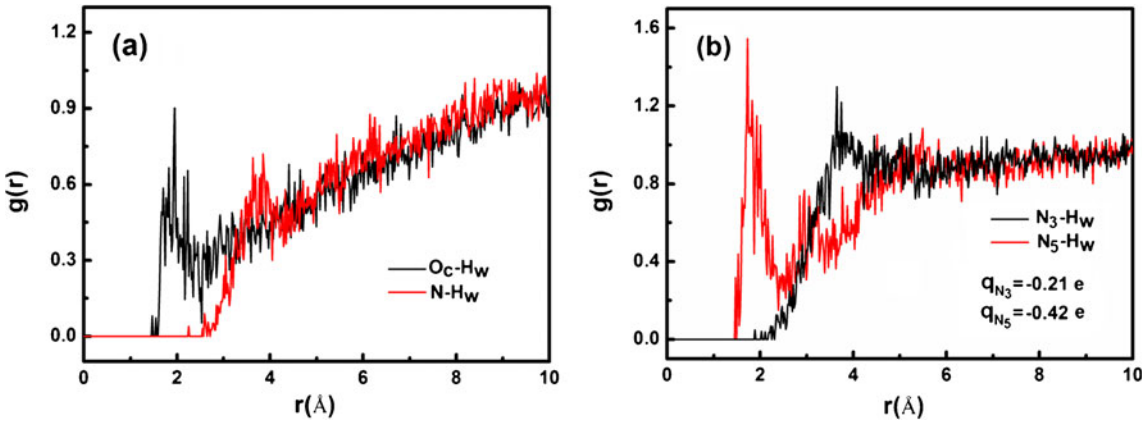


**Fig. 8** The RDF profiles between (**a**) the $O_C$/N atoms of the backbone, (**b**) $N_3$/$N_5$ atoms in side chains of the cyclo-(HH)$_3$ peptide and $H_w$ atoms of water molecules. The atomic numbering can be seen from the note in Fig. 7

numbered clockwise. The water/cyclohexane interface locates obviously at $z$=21.49 Å. The distinct waveform distributions of the solvents in the profiles are probably owed to the added graphene layer.

The cyclo-(GG)$_3$ peptide with no side chain locates basically at the water/cyclohexane interface (Fig. 7a). By contrast, the cyclo-(AA)$_3$ peptide with the methyl (−$CH_3$) side chains moves into the cyclohexane phase slightly (Fig. 7b). The side chains of the cyclo-(DD)$_3$, cyclo-(EE)$_3$, cyclo-(NN)$_3$ and cyclo-(KK)$_3$ peptides tend to insert into the aqueous solution. These four peptides possess hydrophilic –COOH or −$NH_2$ moieties. With the length increasing of the side chains, hydroxyls in the cyclo-(DD)$_3$ and cyclo-(EE)$_3$ peptides go into water phase deeper (Fig. 7c and d). It happens also for the −$NH_2$ groups in the cyclo-(NN)$_3$ and cyclo-(KK)$_3$ peptides (Fig. 7e and f). The average position of −$NH_2$ moiety in the cyclo-(NN)$_3$ peptide locates at the interface region, while that in the cyclo-(KK)$_3$ peptide distinctively moves into water phase. A particular phenomenon can be found for the cyclo-(HH)$_3$ and cyclo-(PP)$_3$ peptides that there is no separation between the distributions of the backbones and those of the side chains (Fig. 7g and h), owing to the special amino acid residues in these two CHPs. The results coincide with the orientation distributions of **CC**, **NN** and **SC** vectors in Figs. 4, 5 and 6. The backbones of the cyclo-(CC)$_3$ and cyclo-(FF)$_3$ peptides both migrate to the cyclohexane phase. –SH moiety and $C_1$, $C_4$ atoms in the side chains all insert into the cyclohexane phase (Fig. 7i and j), resulted from the strong hydrophobicity of –SH and –$CH_2$-Ph, respectively.

The nature of the interactions between the CHPs and water molecules was further investigated by radial distribution functions (RDFs). As examples, the results of the cyclo-(HH)$_3$ and cyclo-(FF)$_3$ peptides were shown in Figs. 8 and 9, respectively. RDF analyses of Figs. 8a and 9a show that the H-bonds were formed between the $O_C$ atoms of the CHPs' backbones and $H_w$ atoms of water molecules, which are stable even at high temperature (353 K). Nevertheless, N atoms of the CHPs' backbones form the H-bonds or van der Waals interactions with the water solvent (Figs. 8a and 9b). The interactions between the side chains and water phase exist in the forms of H-bonds or van der Waals interactions (Fig. 8b).

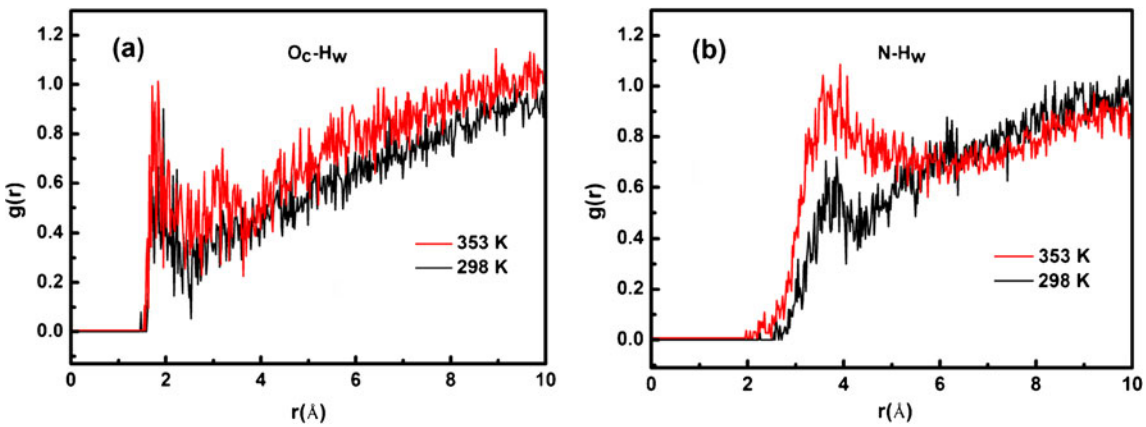


**Fig. 9** The RDF profiles between the (**a**) $O_C$, (**b**) N atoms of the backbone of the cyclo-(FF)$_3$ peptide and $H_w$ atom of water molecules at 298 and 353 K, respectively

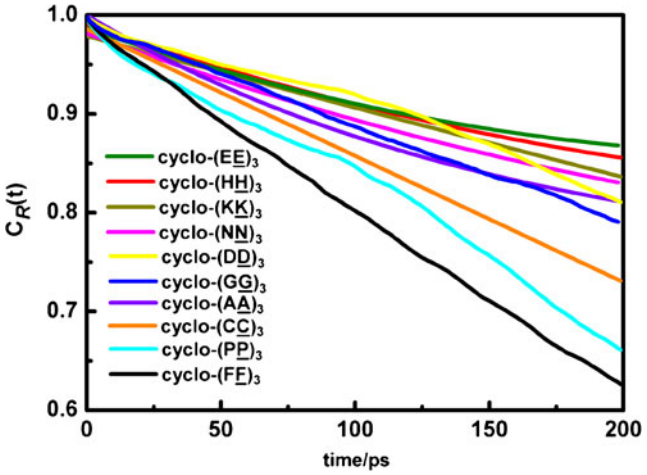


**Fig. 10** Reorientational dynamics [$C_{\mathbf{R}}(t)$] of the CHP backbones, computed by averaging the reorientational time correlation functions of six vectors (i.e., 3 **CC** and 3 **NN** vectors) based on Eq. 3

## Dynamic properties of CHPs at the water/cyclohexane interface

Dynamic characteristics of CHPs was studied by investigating the translational mobilities and rotational activities of CHPs at the water/cyclohexane interface. The formers were done by the computation of the molecular diffusion coefficients ($D$) by directly measuring the mean square displacements (MSD) of the centers of CHP backbones according to the following Einstein relation [29],

$$D = \lim_{\Delta t=\infty} \frac{\langle |r_i(t) - r_i(0)| \rangle^2}{2d\Delta t} = \lim_{t\to\infty} \frac{\langle \Delta r^2 \rangle}{2d\Delta t} \quad (2)$$

where $d$ is the dimension. The diffusion of the adsorbed CHPs at the water/cyclohexane interface is anisotropic. Owing to the complexity of the potential surfaces in z-axis direction, the mean-square-displacement data are not directly related to the diffusion constant in this direction [32]. We mainly investigated the MSDs of the CHPs in the $xy$ plane (i.e., at the interface), corresponding to the lateral diffusion coefficients $D_{xy}$ [29]. The results are included in Table 1. The lateral diffusion coefficients ($D_{xy}$) range from 3.298 to $3.786\times10^{-6}$ cm$^2$·s$^{-1}$. The cyclo-(DD)$_3$, cyclo-(EE)$_3$, cyclo-(NN)$_3$ and cyclo-(KK)$_3$ peptides with the hydrophilic side chains display relatively slower diffusion than those with the hydrophobic ones, such as the cyclo-(CC)$_3$, cyclo-(AA)$_3$, cyclo-(FF)$_3$ and cyclo-(PP)$_3$ peptides. The cyclo-(EE)$_3$ peptide moves the slowest and the cyclo-(FF)$_3$ one ranks ahead.

The rotational activities of CHPs reflect the reorientational dynamics of the backbones. The reorientational time correlation function of the vector **R** was calculated by [33]

$$C_{\mathbf{R}}(t) = \frac{\langle \mathbf{R}(\tau) \cdot \mathbf{R}(t+\tau) \rangle}{\langle \mathbf{R}(\tau) \cdot \mathbf{R}(\tau) \rangle} \quad (3)$$

The final reorientational dynamics of a CHP backbone was obtained by averaging the reorientational time correlation functions of six vectors (i.e., 3 **CC** and 3 **NN** vectors). The results are shown in Fig. 10. It can be found that the relaxational motions of the cyclo-(HH)$_3$, cyclo-(EE)$_3$, cyclo-(NN)$_3$ and cyclo-(DD)$_3$ peptides are the slowest. However, the cyclo-(FF)$_3$ peptide with the strong hydrophobic side chain relaxes the fastest. In a word, the strong interactions between the hydrophilic groups of the residues and water molecules slow down the reorientational motions of CHPs at the interface.

## Water dynamics in the interfacial region and near the graphene wall

To obtain a more complete microscopic description and to understand the dynamics of an adsorbed CHP at the interface, one should investigate the dynamics of water molecules in the vicinity of CHP. Taking into account that the introduced graphene wall definitely influences the dynamic characteristics of the nearby water, this part focuses on the dynamics of water molecules in the range of 5 Å along $z$ direction in the region of the water/cyclohexane interface and near the graphene wall. Owing to the presence of the graphene wall and water/cyclohexane interface, the mean-square-displacement data in the z-axis direction of water

**Table 2** The lateral translational diffusion coefficients ($D_{xy}$ in $10^{-5}$ cm$^2$·s$^{-1}$) of the water molecules in the region of the water/cyclohexane interface and near the graphene wall

| CHPs | In the region of the water/cyclohexane interface | Near the graphene wall |
|---|---|---|
| Cyclo-(FF)$_3$ peptide | 2.125 | 2.515 |
| Cyclo-(PP)$_3$ peptide | 2.124 | 2.585 |
| Cyclo-(CC)$_3$ Ceptide | 2.010 | 2.561 |
| Cyclo-(AA)$_3$ peptide | 2.066 | 2.574 |
| Cyclo-(GG)$_3$ peptide | 2.270 | 2.531 |
| Cyclo-(DD)$_3$ peptide | 2.005 | 2.569 |
| Cyclo-(NN)$_3$ peptide | 1.989 | 2.583 |
| Cyclo-(HH)$_3$ peptide | 1.968 | 2.536 |
| Cyclo-(KK)$_3$ peptide | 1.954 | 2.552 |
| Cyclo-(EE)$_3$ peptide | 1.885 | 2.575 |

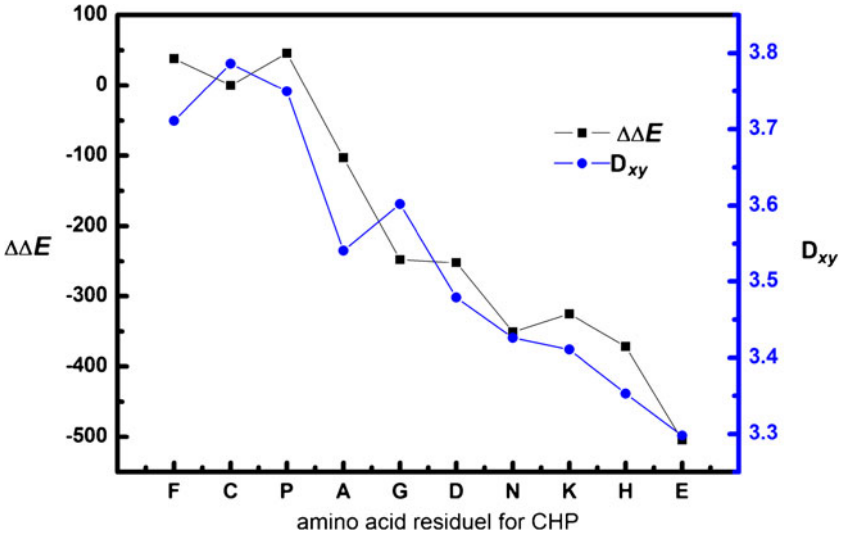


**Fig. 11** Relationship between the lateral diffusion coefficients ($D_{xy}$, in $10^{-6}cm^2 \cdot s^{-1}$) of CHPs at the water/cyclohexane interface and the differences ($\Delta\Delta E$, in $kJ \cdot mol^{-1}$) of the interaction energies between CHPs and two solvents. $\Delta\Delta E = \Delta E_1 - \Delta E_2$. $\Delta E_1$ donates the interaction energy between a CHP and water phase, and $\Delta E_2$ that between a CHP and cyclohexane phase

molecules are not directly related to the diffusion constant in this direction [29]. We mainly investigated the lateral translational motions ($D_{xy}$) of water molecules. The results are listed in Table 2. On the removal of the graphene wall, CHP and cyclohexane molecules in a modeling system, the diffusion coefficient of the remaining water molecules was calculated as $2.68 \times 10^{-5} cm^2 \cdot s^{-1}$, quite consistent with the reported result [34]. It is evident that the translational motions of the hydration layer water in these two vicinities are restricted more or less as compared to that of the pure bulk water. It is clearly shown that the artificially introduced graphene wall in our simulation systems has little influence on the diffusion of water molecules. The movements of water molecules close to the water/cyclohexane interface are much more confined. It can be found that the strong interactions between the water molecules and the hydrophilic head groups of the side chains of CHPs further weaken the diffusion of water molecules at the water/cyclohexane interface. The results indicate that the dynamics of the CHPs and interfacial water molecules are strongly coupled.

## Interactions between CHPs and solvents

The interaction energy ($\Delta E$) between a CHP and a solvent phase was defined as:

$$\Delta E = E_{CHP+Solvent} - (E_{CHP} + E_{solvent}) \quad (4)$$

where $E_{CHP+solvent}$, $E_{CHP}$ and $E_{solvent}$ denote the energies of the whole system on condition of removing the graphene wall and another solvent phase, a CHP molecule and a solvent phase (water or cyclohexane), obtained by a self-programmed software. The results are contained in Table 3. $\Delta E_1$ represents the interaction energy between a CHP molecule and water phase. $\Delta E_2$ stands for that between a CHP molecule and cyclohexane phase. Obviously, the cyclo-(E$\underline{\text{E}}$)$_3$ and cyclo-(P$\underline{\text{P}}$)$_3$ peptides have the largest $|\Delta E_1|$ and $|\Delta E_2|$, respectively. $\Delta\Delta E$ is the difference of $\Delta E_1$ and $\Delta E_2$, reflecting the contention of the water and cyclohexane phases on a CHP molecule. Obviously, such quantity is critical to the dynamic characteristics of a CHP molecule at the water/cyclohexane interface. Figure 11 shows the relationships between $\Delta\Delta E$ and the lateral diffusion coefficients ($D_{xy}$) of CHPs. There is a certain correlation between $D_{xy}$ and $\Delta\Delta E$. The main abnormality is found for the cyclo-(C$\underline{\text{C}}$)$_3$ and cyclo-(G$\underline{\text{G}}$)$_3$ peptides. The former has nearly the same interactions with the water and cyclohexane phases. Compared with cyclo-(D$\underline{\text{D}}$)$_3$, cyclo-(G$\underline{\text{G}}$)$_3$ has a similar $\Delta\Delta E$ but much larger $D_{xy}$. The reason is probably that the cyclo-(G$\underline{\text{G}}$)$_3$ peptide is the smallest in all (Table S2), resulting in its rapid molecular movement at the interface. Therefore, it can be inferred that molecular volume is also a fact influencing molecular diffusion at the interface.

**Table 3** The interaction energies ($\Delta E_1$ and $\Delta E_2$ in $kJ \cdot mol^{-1}$) between CHPs and one of the two solvents (water or cyclohexane) and their differences ($\Delta\Delta E$)[a]

| CHPs | $\Delta E_1$ | $\Delta E_2$ | $\Delta\Delta E$ |
|---|---|---|---|
| Cyclo-(E$\underline{\text{E}}$)$_3$ peptide | −589.67 | −85.20 | −504.47 |
| Cyclo-(H$\underline{\text{H}}$)$_3$ peptide | −525.69 | −154.07 | −371.62 |
| Cyclo-(K$\underline{\text{K}}$)$_3$ peptide | −496.68 | −171.28 | −325.40 |
| Cyclo-(N$\underline{\text{N}}$)$_3$ peptide | −460.34 | −109.40 | −350.94 |
| Cyclo-(D$\underline{\text{D}}$)$_3$ peptide | −412.82 | −161.07 | −251.75 |
| Cyclo-(G$\underline{\text{G}}$)$_3$ peptide | −335.66 | −88.09 | −247.57 |
| Cyclo-(A$\underline{\text{A}}$)$_3$ peptide | −216.25 | −113.29 | −102.95 |
| Cyclo-(F$\underline{\text{F}}$)$_3$ peptide | −210.01 | −248.15 | 38.14 |
| Cyclo-(C$\underline{\text{C}}$)$_3$ peptide | −186.40 | −186.10 | −0.29 |
| Cyclo- (P$\underline{\text{P}}$)$_3$ peptide | −161.99 | −207.83 | 45.85 |

[a] $\Delta\Delta E = \Delta E_1 - \Delta E_2$. $\Delta E_1$ donates the interaction energy between a CHP and water phase, and $\Delta E_2$ that between a CHP and cyclohexane phase

## Conclusions

The effects of the side chains on the structures, orientations and dynamics of ten CHPs at the water/cyclohexane interface were studied by all atomistic MD simulations. All the CHPs take the "horse-saddle" structures at the interface and the diverse hydrophilicity/hydrophobicity of the side chains results in different degrees of CHP backbone deformations. The cyclo-(P$\underline{P}$)$_3$, cyclo-(F$\underline{F}$)$_3$ and cyclo-(H$\underline{H}$)$_3$ peptides deform little owing to their ring structures of the side chains. The smallest cyclo-(G$\underline{G}$)$_3$ peptide with no side chain exhibits the biggest deformation. The backbones of CHPs display tilting at the water/cyclohexane interface and the flexible side chains fold back to interact with the backbones. The H-bonds were formed between the $O_C$ atoms of the CHPs' backbones and water molecules. Nevertheless, N atoms of the CHPs' backbones formed the H-bonds or van der Waals interactions with the water solvent. The lateral translational and rotational motions of CHPs at the interface were largely slowed down by the strong polar interactions between the CHPs and water molecules. There is a certain correlation between the lateral diffusion coefficient ($D_{xy}$) of a CHP in the interface plane and the differences ($\Delta\Delta E$) of the interaction energies of a CHP with the two solvents. The lateral translational activities of water near the graphene wall and in the region of the water/cyclohexane interface were confined more or less by the graphene layer, the biphasic interface and the introduced CHPs, respectively. The results indicate the dynamics of the CHPs and interfacial water molecules are strongly coupled. The simulations present direct information of the structural and dynamical properties of CHPs at the water/cyclohexane interface, and the results will be helpful for better understanding of the hydrophilic/hydrophobic properties of the CHPs.

**Acknowledgments** This work has been supported by the National Natural Science Foundation of China (Grant No. 21173154) and the Priority Academic Program Development of Jiangsu Higher Education Institutions. The authors are grateful to College of Computer Science & Technology in Soochow University for providing amounts of computer facilities assignment on its high-powered computers.

## References

1. Vollenbroich D, Ozel M, Vater J, Kamp RM, Pauli G (1997) Mechanism of inactivation of enveloped viruses by the biosurfactant surfactin from bacillus subtilis. Biologicals 25:289–297
2. Kracht M, Rokos H, Ozel M, Kowall M, Pauli G, Vater J (1999) Antiviral and hemolytic activities of surfactin isoforms and their methyl ester derivative. J Antibiot 52:613–619
3. Tendulkar SR, Saikumari YK, Patel V, Raghotama S, Munshi TK, Balaram P, Chattoo BB (2007) Isolation, purification and characterization of an antifungal molecule produced by bacillus licheniformis BC98, and its effect on phytopathogen magnaporthe grise. J Appl Microbiol 103:2331–2339
4. Weber C, Wider G, von Freyberg B, Traber R, Braun W, Widmer H, Wuthrich K (1991) The NMR structure of cyclosporin a bound to cyclophilin in aqueous solution. Biochemistry 30:6563–6574
5. Trevisan G, Maldaner G, Velloso NA, Sant'Anna GS, Ilha V, Gewehr CCV, Rubin MA, Morel AF, Ferreira J (2009) Antinociceptive effects of 14-membered cyclopeptide alkaloids. J Nat Prod 72:608–612
6. Gang HZ, Liu JF, Mu BZ (2010) Molecular dynamics simulation of Surfactin derivatives at the decane/water interface at Low surface coverage. J Phys Chem B 114:2728–2737
7. Liu J, Fan JF, Tang M, Zhou WQ (2010) Molecular dynamics simulation for the structure of the water chain in a transmembrane peptide nanotube. J Phys Chem A 114:2376–2383
8. Bagheri M, Keller S, Dathe M (2011) Interaction of W-substituted analogs of cyclo- RRRWFW with bacterial lipopolysaccharides: the role of the aromatic cluster in antimicrobial activity. Antimicrob Agents Chemother 55:788–797
9. Jelokhani-Niaraki M, Kondejewski LH, Wheaton LC, Hodges RS (2009) Effect of ring size on conformation and biological activity of cyclic cationic antimicrobial peptides. J Med Chem 52:2090–2097
10. Praveena G, Kolandaivel P (2008) Structural and dynamical studies of all-trans and all-cis Cyclo[(1R,3S)-$\gamma$-Acc-Gly]$_3$ peptides. J Mol Model 14:1147–1157
11. Praveena G, Kolandaivel P (2009) Interaction of metal ions with Cyclo[(1R,3S)-c-Acc-Gly]$_3$ Hexapeptide –a theoretical study. J Mol Struct (THEOCHEM) 900:96–102
12. Leodidis EB, Hatton TA (1990) Amino acids in AOT reversed Micelles. 2. The hydrophobic effect and hydrogen bonding as driving forces for interfacial solubilization. J Phys Chem 94:6411–6420
13. Wolfenden R, Andersson L, Cullis PM, Southgate CCB (1981) Affinities of amino acid side chains for solvent water. Biochemistry 20:849–855
14. Horinek D, Netz RR (2011) Can simulations quantitatively predict peptide transfer free energies to urea solutions? thermodynamic concepts and force field limitations. J Phys Chem A 115:6125–6136
15. Nicolas JP (2003) Molecular dynamics simulation of surfactin molecules at the water- hexane interface. Biophys J 85:1377–1391
16. Bonmatin JM, Genest M, Labbe H, Ptak M (1994) Solution three-dimensional structure of surfactin: a cyclic lipopeptide studied by 1 H-NMR, distance geometry, and molecular dynamics. Biopolymers 34:975–986
17. Gallet X, Deleu M, Razafindralambo H et al (1999) Computer simulation of surfactin conformation at a hydrophobic/hydrophilic interface. Langmuir 15:2409–2413
18. Gang HZ, Liu JF, Mu BZ (2010) Interfacial behavior of surfactin at the decane/water interface: a molecular dynamics simulation. J Phys Chem B 114(46):14947–14954
19. Ahmad F, Constabel F, Geckler KE, Seeck OH, Seo YS et al (2005) X-ray reflectivity study of cyclic peptide monolayers at the air–water interface. Israel J Chem 45:345–352
20. Ulmschneider JP, Smith JC, White SH, Ulmschneider MB (2011) In silico partitioning and transmembrane insertion of hydrophobic peptides under equilibrium conditions. J Am Chem Soc 133:15487–15495
21. Khurana E, DeVane RH, Kohlmeyer A, Klein ML (2008) Probing peptide nanotube self-assembly at a liquid-liquid interface with coarse-grained molecular dynamics. Nano Lett 8:3626–3630
22. Rapaport H, Kim HS, Kiaer K et al (1999) Crystalline cyclic peptide nanotubes at interfaces. J Am Chem Soc 121:1186–1191
23. Ghadiri MR, Granja JR, Milligan RA, Duncan EM, Khazanovich N (1993) Self-assembling organic nanotubes based on a cyclic peptide architecture. Nature 366:324–327
24. Liu J, Fan JF, Tang M, Cen M, Yan JF et al (2010) Water diffusion behaviors and transportation properties in transmembrane cyclic hexa-, octa- and decapeptide nanotubes. J Phys Chem B 114:12183–12192

25. Sun H (1998) COMPASS: an ab initio force-field optimized for condensed-phase applications-overview with details on alkane and benzene compounds. J Phys Chem B 102:7338–7364
26. McCool MA, Woolf LA (1972) Self-diffusion measurements under pressure with a diaphragm cell. Theory of the method and experimental results for cyclohexane. High Temp-High Press 4:85–95
27. Nose S (1984) A molecular dynamics method for simulations in the Canonocal ensemble. Mol Phys 52:255–268
28. Berendsen HJC, Postma JPM, van Gunsteren WE et al (1984) Molecular dynamics with coupling to an external bath. J Chem Phys 81:3684–3692
29. Allen MP, Tildesley DJ (1989) Computer simulation of liquids. Clarendon, Oxford
30. Smith W (1992) A replicated data molecular dynamics strategy for the parallel Ewald Sum. Comput Phys Commun 67:392–406
31. Pang JY, Wang YJ, Xu GY, Han TT (2011) Molecular dynamics simulations of SDS, DTAB, and C12E8 monolayers adsorbed at the air/water surface in the presence of DSEP. J Phys Chem B 115:2518–2526
32. Sedlmeier F, von Hansen Y, Mengyu L, Horinek D, Netz RR (2011) Water dynamics at interfaces and solutes: disentangling free energy and diffusivity contributions. J Stat Phys 145:240–252
33. Jang SS, Goddard WA (2006) Structures and properties of Newton black films characterized using molecular dynamics simulations. J Phys Chem B 110:7992–8001
34. Mark P, Nilsson L (2001) Structure and dynamics of the TIP3P, SPC, and SPC/E water models at 298 K. J Phys Chem A 105:9954–9960